

# Novel Cytotoxic Copper(II) Complexes of 8-Aminoquinoline Derivatives: Crystal Structure and Different Reactivity towards Glutathione

Shouchun Zhang,<sup>[a]</sup> Chao Tu,<sup>[a]</sup> Xiongyong Wang,<sup>[a]</sup> Zhen Yang,<sup>[a]</sup> Junyong Zhang,<sup>[a]</sup>  
Liping Lin,<sup>[b]</sup> Jian Ding,<sup>[b]</sup> and Zijian Guo<sup>\*[a]</sup>

**Keywords:** Antitumor agents / Bioinorganic chemistry / Copper / N ligands

Two novel Cu<sup>II</sup> complexes [Cu(CMQA)(H<sub>2</sub>O)] (**1**) (CMQA = *N*-carboxymethyl-L-methionine-*N'*-8-quinolylamide) and [Cu(MQA)(OAc)] (**2**) (MQA = L-methionine-*N'*-8-quinolylamide, OAc = CH<sub>3</sub>COO<sup>-</sup>) have been synthesized and structurally characterized. Complex **1** crystallizes in the orthorhombic system with space group *P*2<sub>1</sub>2<sub>1</sub>2<sub>1</sub> [*a* = 5.556(1) Å, *b* = 15.002(3) Å, *c* = 20.886(4) Å] while complex **2** crystallizes in the monoclinic system with space group *C*2 [*a* = 28.463(6) Å, *b* = 5.264(1) Å, *c* = 13.345(3) Å, β = 109.142(3)°]. In both complexes the Cu<sup>II</sup> center is coordinated by three N atoms of the ligand and one O atom of H<sub>2</sub>O (**1**) or OAc (**2**). The in vitro cytotoxicity of both complexes and their corresponding li-

gands have been tested against the murine leukemia P-388 and lung adenocarcinoma A-549 cell lines. Complex **2** shows a potent activity against both cell lines with an inhibitory rate of 100% for the murine leukemia P-388 cell line and 93.4% for the lung adenocarcinoma A-549 cell line at a concentration of 10<sup>-6</sup> mol·L<sup>-1</sup>, while complex **1** shows only a marginal activity against the same cell lines. The reactivity of the two complexes towards γ-glutathione (GSH) has been investigated and is discussed in association with their different cytotoxicity.

(© Wiley-VCH Verlag GmbH & Co. KGaA, 69451 Weinheim, Germany, 2004)

## Introduction

The application of metal complexes in medicine has become increasingly prevalent since the clinical success of cisplatin for treatment of several human malignant tumors decades ago.<sup>[1–4]</sup> Copper has a long history of medical use, and its potential antitumor properties have attracted attention recently because it is thought to be less toxic than non-essential metals such as platinum.<sup>[5]</sup> For example, Cu<sup>II</sup> complexes of thiosemicarbazone are a family of the most promising non-platinum compounds with antitumor potential.<sup>[6–8]</sup> Some tertiary Cu<sup>II</sup>-amino acid-phenanthroline complexes (Casiopinas) exhibit high antitumor activity towards a variety of tumor cell lines.<sup>[9,10]</sup> More recently, some Cu<sup>II</sup> complexes with macrocyclic ligands<sup>[11,12]</sup> or nitrogen-containing heterocyclic ligands<sup>[13,14]</sup> have also been reported to show potent antitumor activities.

As a part of our interest in the design of quinoline-based metallo-antitumor complexes,<sup>[15–17]</sup> we describe here the

crystal structure and in vitro cytotoxicity of two novel copper complexes [Cu(CMQA)(H<sub>2</sub>O)] (**1**) and [Cu(MQA)(OAc)] (**2**; Scheme 1). The interactions of complexes **1** and **2** with γ-glutathione (GSH) have been studied and the implications for their cytotoxicity are discussed.

## Results and Discussion

### Synthesis

The reaction of Cu(OAc)<sub>2</sub>·H<sub>2</sub>O with ligands **L** and **L'** resulted in two related complexes **1** and **2** (Scheme 1). In the reaction of **L** with Cu(OAc)<sub>2</sub>·H<sub>2</sub>O, the OC(CH<sub>3</sub>)<sub>3</sub> group of **L** is replaced by OCH<sub>3</sub> from the solvent methanol. This ester-exchange reaction has been reported previously in similar reactions.<sup>[17]</sup> During Cu<sup>II</sup> coordination all the amide groups of the ligands are deprotonated, giving rise to a stable delocalized electronic system.<sup>[18,19]</sup> Complex **1** dissolves readily in CH<sub>3</sub>OH, DMSO, and DMF but barely in H<sub>2</sub>O, while complex **2** can dissolve fairly well both in organic solvents such as CH<sub>3</sub>OH, DMSO, DMF and in water.

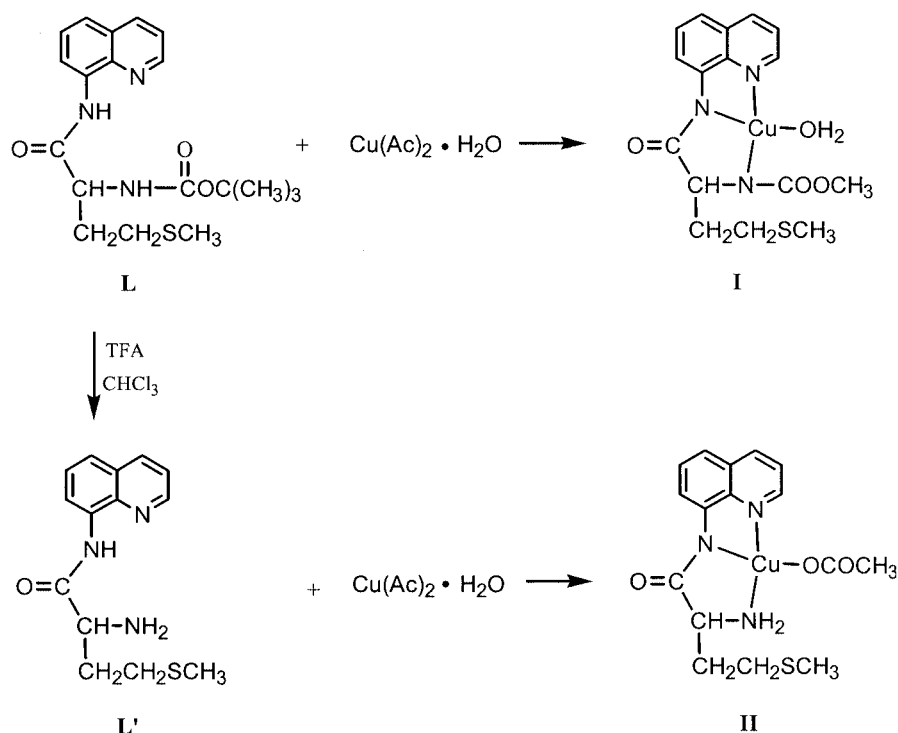
### Structures

The crystal data, data collection, structural solution and refinement parameters for ligand **L** and complexes **1** and **2** are summarized in the Exp. Sect; selected bond lengths and angles are listed in Table 1. The crystal structure of ligand **L** is shown in Figure 1. All the bond lengths and bond

<sup>[a]</sup> State Key Laboratory of Coordination Chemistry, Coordination Chemistry Institute, Nanjing University, Nanjing 210093, P. R. China  
Fax: +86-25-8331-4502  
E-mail: zguo@nju.edu.cn

<sup>[b]</sup> Division of Anti-tumor Pharmacology, State Key Laboratory for New Drug Research, Shanghai Institute of Materia Medica, Shanghai Institute of Biological Science, Shanghai 200031, P. R. China

Supporting information for this article is available on the WWW under <http://www.eurjoc.irg> or from the author.



Scheme 1

angles of **L** are within the normal ranges. The N(2)–C(8) and N(2)–C(10) bond lengths are similar to those of similar ligands.<sup>[20,21]</sup> The crystal packing of ligand **L** is shown in Figure S1. The distance between the two adjacent quinoline planes is 3.390 Å, suggesting the presence of strong intermolecular  $\pi$ - $\pi$  stacking interactions between the adjacent molecules. Intermolecular hydrogen bonds between the hydrogen atom on N(1) and the O(2) atom of a neighboring molecule are observed. The D $\cdots$ A separation is 2.968 Å for N(1) $\cdots$ O(2) (symmetry code:  $x + 1, y, z$ ) and the D–H $\cdots$ A angle is about 156.72° for N(1)–H(1A) $\cdots$ O(2). The crystal structures of complexes **1** and **2** are shown in Figure 2 and 3, respectively. In both complexes the ligand acts as a tridentate chelator coordinated to Cu<sup>II</sup> through the quinolyl N(3) and amide N(1) and N(2) atoms. The fourth coordination position of Cu<sup>II</sup> is occupied by either a water molecule through O(1W) in complex **1** or an acetate through O(2) in complex **2**. In general, the Cu–N<sub>amido</sub> and Cu–N<sub>quinolyl</sub> bond lengths and the bond angles in **1** and **2** are similar to those of related complexes.<sup>[17]</sup> The bond angles show that the geometry around Cu<sup>II</sup> is slightly distorted from the regular square-planar geometry in both complexes. For example, the N(1)–Cu(1)–N(3) and N(2)–Cu(1)–O(1W or 2) angles are contracted from the ideal value of 180° for a regular square-planar structure. Such distortion is often observed in Cu<sup>II</sup> complexes of tridentate chelating agents.<sup>[22–24]</sup> It is notable that the CuN<sub>3</sub>O [Cu(1), N(1), N(2), N(3), O(1W) (for **1**) or O(2) (for **2**)] plane is nearly co-planar with the quinoline ring in both complexes (see Figure S2 and Figure S3 in the Supporting Information for this article; see also the footnote on the

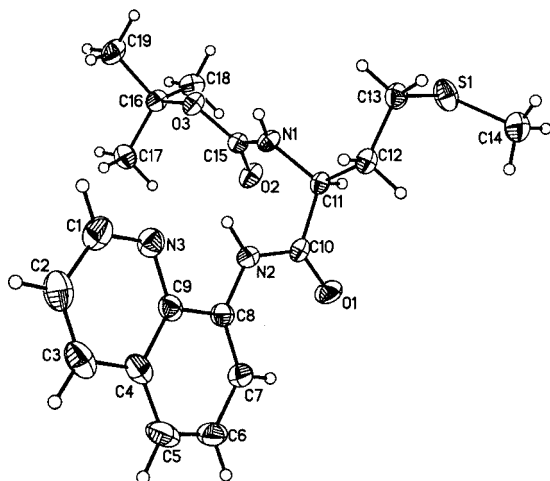
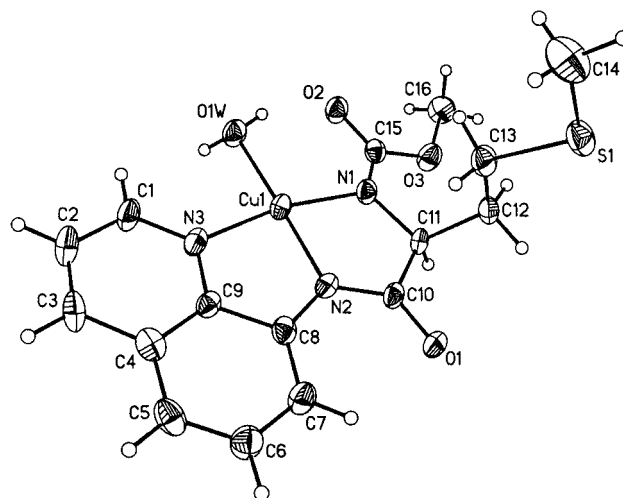
first page of this article), and the mean deviation from the large best plane is 0.004 Å for **1** and 0.026 Å for **2**. There are strong intermolecular  $\pi$ - $\pi$  stacking interactions between the adjacent molecules in both complexes, and the distance between the adjacent planes is 3.506 Å for **1** and 3.574 Å for **2**. There is an intramolecular hydrogen bond (Table S1) in the crystal structure of complex **1**; the D $\cdots$ A separation is 2.545 Å for O(1W) $\cdots$ O(2). The D–H $\cdots$ A angle is about 151° for O(1W)–H(1WA) $\cdots$ O(2). This intramolecular hydrogen bond may be responsible for the poor solubility of complex **1** in water. Intermolecular hydrogen bonds are observed in complex **2** between the hydrogen atoms of the solvent water molecule and N(1) and O(3). No intramolecular hydrogen bond is observed in **2**.

### Cytotoxic Activity

The in vitro cytotoxicity of ligands **L** and **L'** and their copper complexes **1** and **2** was evaluated against the murine leukemia P-388 and lung adenocarcinoma A-549 cell lines with cisplatin as a positive control. The cytotoxicity profiles are shown in Figure 4. The results indicate that the inhibitory rates of complexes **1** and **2** are significantly higher than those of ligands **L** and **L'**, which are inactive to the tested cell lines. This observation is in accordance with the general phenomenon that copper complexes demonstrate enhanced biological activity than their parent ligands.<sup>[25,26]</sup> Complex **2** is far more active than complex **1** against both cell lines under the same conditions, with the latter being active only at concentrations as high as 10<sup>−4</sup> mol·L<sup>−1</sup>. At a concentration of 10<sup>−6</sup> mol·L<sup>−1</sup>, complex **2** still retains a high in-

Table 1. Selected bond lengths (Å) and angles (°) of ligand **L** and complexes **1** and **2**

Ligand <b>L</b>					
N(2)–C(10)	1.356(4)	N(2)–C(8)	1.400(4)	N(3)–C(11)	1.447(4)
C(10)–C(11)	1.531(4)	C(11)–C(12)	1.534(4)	O(1)–C(10)	1.208(4)
C(10)–N(2)–C(8)	128.0(3)	O(1)–C(10)–N(2)	124.8(3)	N(3)–C(11)–C(10)	113.4(2)
N(2)–C(8)–C(9)	115.0(3)	N(2)–C(10)–C(11)	114.5(3)	N(3)–C(9)–C(8)	117.7(3)
Complex <b>1</b>					
Cu(1)–N(1)	1.939(7)	Cu(1)–N(2)	1.906(6)	Cu(1)–N(3)	1.986(7)
Cu(1)–O(1W)	1.949(5)	N(3)–C(1)	1.328(10)	N(3)–C(9)	1.372(10)
N(2)–C(10)	1.334(9)	N(2)–C(8)	1.386(10)	C(8)–C(9)	1.443(10)
N(1)–C(11)	1.481(9)	N(1)–C(15)	1.308(10)	O(1)–C(10)	1.232(9)
N(1)–Cu(1)–N(3)	167.5(2)	N(1)–Cu(1)–O(1W)	97.0(2)	N(2)–Cu(1)–O(1W)	178.4(3)
N(2)–Cu(1)–N(3)	83.1(3)	N(2)–Cu(1)–N(1)	84.4(3)	C(11)–N(1)–Cu(1)	113.3(5)
C(10)–N(2)–Cu(1)	117.9(5)	C(8)–N(2)–Cu(1)	115.3(5)	C(1)–N(3)–Cu(1)	129.9(6)
C(9)–N(3)–Cu(1)	112.7(5)	O(1W)–Cu(1)–N(3)	95.4(2)	C(15)–N(1)–Cu(1)	125.4(5)
Complex <b>2</b>					
Cu(1)–N(1)	2.017(8)	Cu(1)–N(2)	1.887(8)	Cu(1)–N(3)	1.993(8)
Cu(1)–O(2)	1.923(8)	N(3)–C(1)	1.313(14)	N(3)–C(9)	1.357(15)
N(2)–C(10)	1.350(12)	N(2)–C(8)	1.400(13)	C(8)–C(9)	1.456(15)
N(1)–C(11)	1.502(13)	O(1)–C(10)	1.202(14)	O(2)–C(15)	1.225(15)
N(1)–Cu(1)–N(3)	167.7(4)	N(1)–Cu(1)–O(2)	101.0(3)	N(2)–Cu(1)–O(2)	173.7(4)
N(2)–Cu(1)–N(3)	83.3(4)	N(2)–Cu(1)–N(1)	84.4(3)	C(11)–N(1)–Cu(1)	107.4(6)
C(10)–N(2)–Cu(1)	117.4(7)	C(8)–N(2)–Cu(1)	116.7(7)	C(1)–N(3)–Cu(1)	128.8(8)
C(9)–N(3)–Cu(1)	111.9(7)	O(2)–Cu(1)–N(3)	91.4(4)	C(15)–O(2)–Cu(1)	133.8(8)

Figure 1. Crystal structure of ligand **L** (ORTEP drawing)Figure 2. Crystal structure of complex **1** (ORTEP drawing)

hibitory rate against both the murine leukemia P-388 cell line (100%) and lung adenocarcinoma A-549 cell line (93.4%), and is about two to three times more potent than cisplatin. In fact, the activity of complex **2** is more potent than cisplatin at most experimental concentrations.

### Interactions with DNA and GSH

It is commonly believed that DNA is the main cellular target of metal-based antitumor agents.<sup>[27]</sup> DNA-binding studies were therefore carried out to reveal the potential biological target for complexes **1** and **2**. To our surprise, the

CD data (Figure S3, Supporting Information) do not show significant changes upon addition of the complexes to calf thymus DNA. The UV data (Figure S4, Supporting Information) also suggest that these complexes do not bind to DNA under the experimental conditions studied. This result suggests that another biological target may exist for complexes **1** and **2**.

As one of the most widely distributed intracellular reductants, GSH also plays an important role in metal detoxification.<sup>[28–31]</sup> Recently, a quantitative study has shown that GSH is a crucial contributor to protect against Cu cytotoxicity and it may function both in concert with, or

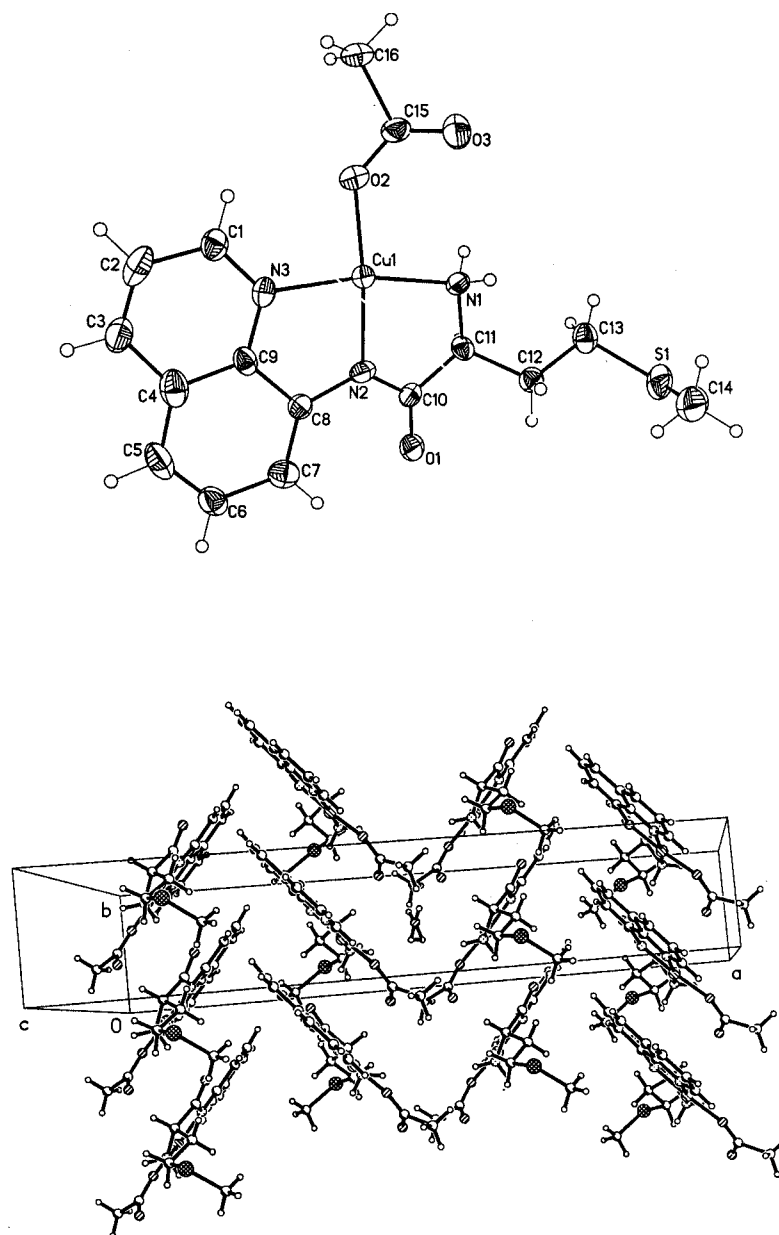


Figure 3. Crystal structure (ORTEP drawing) (top) and structure packed along the *b* axis (bottom) of complex **2**

independently of, metallothionein.<sup>[32]</sup> We thus studied the interaction of complexes **1** and **2** with GSH. As shown in Figure 5, the absorbances of complex **1** at 259 and 365 nm decrease gradually while the absorbances at about 241 and 302 nm increase upon the addition of GSH. When the concentration of GSH was increased to  $3.33 \times 10^{-5} \text{ mol} \cdot \text{L}^{-1}$ , equivalent to that of complex **1**, the absorption bands at 259 and 365 nm disappeared completely. In contrast to complex **1**, no new absorption bands and only inconspicuous absorption changes were observed in the UV spectra upon addition of GSH to a solution of **2**. Interestingly, this result is closely correlated with the cytotoxicity of these complexes. The GSH-reactive complex **1** is biologically inactive against tumor cells, while GSH-inactive complex **2** is biologically active. This relationship between reactivity and

cytotoxicity may result from the Cu detoxification by intracellular GSH. Upon entering tumor cells, complex **1** would react with intracellular GSH and thus prevent it from reaching its desired target and exhibiting cytotoxicity. Complex **2** does not react with GSH, therefore its cytotoxicity in tumor cells is retained. It is therefore tempting to suggest that GSH could be used as a probe to select cytotoxic copper(II) complexes, although many more complexes need to be tested.

The electrochemical behavior of complexes **1** and **2** was also studied to explain the different reactivity of both complexes toward GSH (Figure S5). Complex **2** undergoes a reduction process at about  $-900 \text{ mV}$ , which is far more negative than that of complex **1** (about  $-600 \text{ mV}$ ). The difference in activation energies ( $\Delta G^\ddagger$ ) of both complexes re-

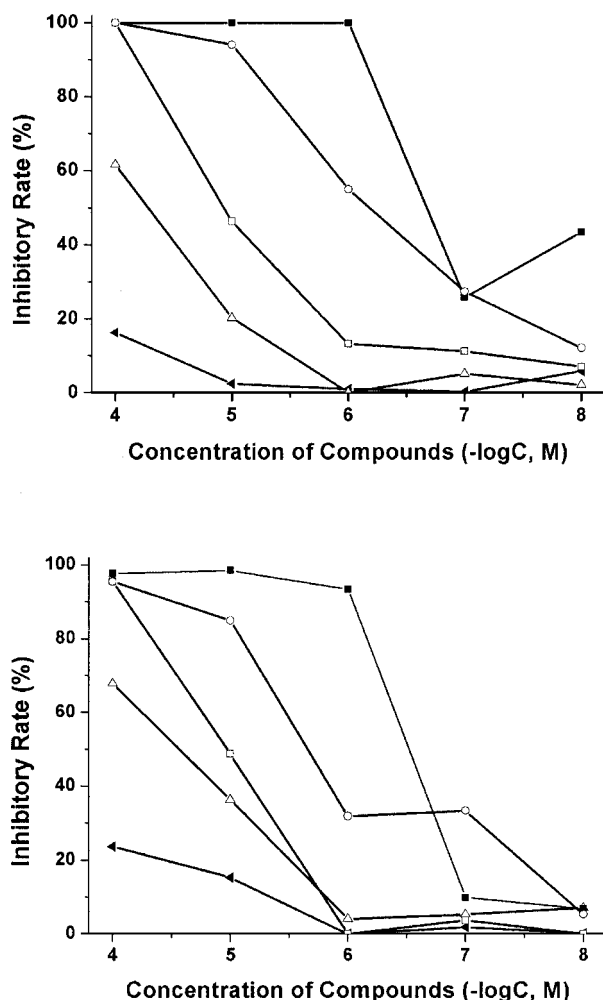


Figure 4. Cytotoxic activity of compounds against murine leukemia P-388 cell line (top) and lung adenocarcinoma A-549 cell line (bottom) (solid triangle: ligand **L**; hollow triangle: ligand **L'**; hollow square: complex **1**; solid square: complex **2**; hollow circle: cisplatin)

duced on the surface of the electrode was about  $29 \text{ kJ} \cdot \text{mol}^{-1}$ , indicating that a higher activation energy is needed to drive the charge-transfer process for complex **2** than for **1**, which is consistent with their different reactivity toward GSH. Additionally, the poor cytotoxicity of complex **1** may also result from its low solubility. The adequate solubility of complex **2** in both organic solvents and water facilitates its transport and absorption in cells, and makes it easier to reach the target.

## Conclusion

Although complex **1** and **2** have similar distorted square-planar configurations, their cytotoxicity and reactivity toward GSH are very different. The in vitro cytotoxicity of complex **2** against murine leukemia P-388 and lung adenocarcinoma A-549 cell lines is more potent than cisplatin at most experimental concentrations, whereas complex **1** only shows a marginal cytotoxicity against the same cells. Com-

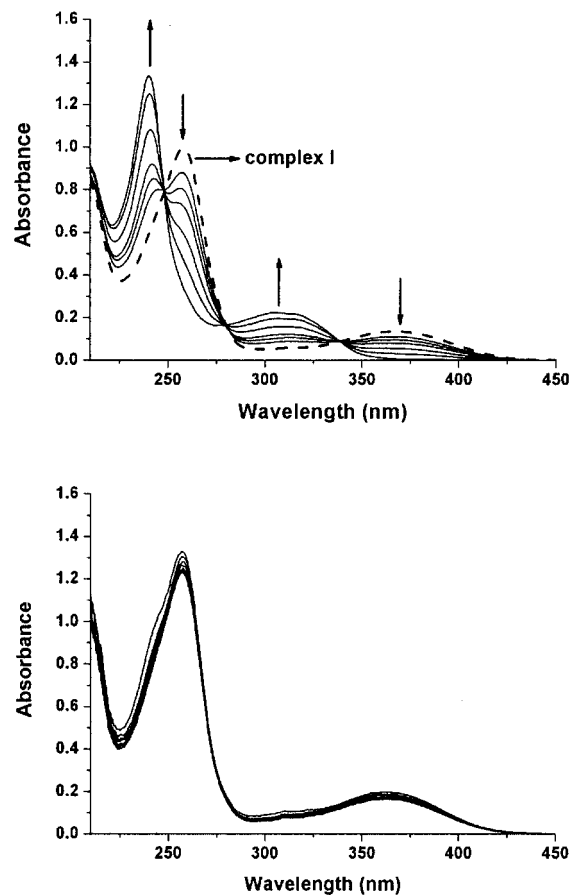


Figure 5. UV absorption spectra of complexes **1** (top) and **2** (bottom) in methanol with increasing concentration of GSH.  $[1] = [2] = 3.33 \times 10^{-5} \text{ mol} \cdot \text{L}^{-1}$ ;  $[\text{GSH}] = 0, 0.55 \times 10^{-5}, 0.83 \times 10^{-5}, 1.11 \times 10^{-5}, 1.67 \times 10^{-5}, 2.22 \times 10^{-5}, 3.33 \times 10^{-5} \text{ mol} \cdot \text{L}^{-1}$ ; the time span between two successive spectra was 10 min

plex **1** is reactive toward GSH while complex **2** is inert. This fact implies that GSH may be used as a useful probe to predict the cytotoxicity of copper complexes.

## Experimental Section

**General Remarks:** Solvents such as methanol, tetrahydrofuran, acetone, anhydrous diethyl ether, chloroform, *N,N*-dimethylformamide (DMF) and common reagents such as  $\text{Cu}(\text{OAc})_2 \cdot \text{H}_2\text{O}$ , triethylamine and trifluoroacetic acid (TFA) were all of analytical grade and used as received. 8-Aminoquinoline and di-*tert*-butyl dicarbonate were purchased from Acros Organics. L-Methionine, the disodium salt of calf thymus DNA (CT DNA) and the reduced  $\gamma$ -glutathione were purchased from Sigma. The infrared spectra were recorded on a Bruker VECTOR22 spectrometer as KBr pellets ( $4000\text{--}500 \text{ cm}^{-1}$ ), and elemental analysis was performed on a Perkin–Elmer 240C analytical instrument. Electrochemical measurements were made at  $20^\circ \text{C}$  on an EG&G PAR Model 273 potentiostat. A three-electrode setup comprising a platinum working electrode, platinum wire auxiliary electrode, and an Ag/AgCl reference electrode was used for voltammetric work. Tetrabutylammonium perchlorate (TBAP) was used as the supporting electrolyte in DMF.



*N*-(*tert*-Butoxycarbonyl)-L-methionine-*N'*-8-quinolylamide (**L**) and its deprotected counterpart L-methionine-*N'*-8-quinolylamide (**L'**) were synthesized following a procedure described previously.<sup>[17]</sup> Colorless single crystals of **L** suitable for X-ray diffraction were obtained by slow evaporation of an acetone solution.

**Complex 1:** This complex was prepared by mixing a methanol solution of Cu(OAc)<sub>2</sub>·H<sub>2</sub>O (0.5 mmol, 6 mL) and **L** (6 mL) in a 1:1 molar ratio. The resulting solution was refluxed for about 2 h, and then cooled to room temperature. Brownish-red single crystals suitable for X-ray diffraction were obtained by slow evaporation of the solvent. Yield 164 mg (80%). C<sub>16</sub>H<sub>19</sub>CuN<sub>3</sub>O<sub>4</sub>S (412.94): calcd. C 45.2, H 4.27, N 10.5; found C 45.5, H 4.33, N 10.4. IR (KBr):  $\tilde{\nu}$  = 3446.8 (m), 3207.9 (m), 1600.7 (s), 1567.6 (s), 1498.3 (m), 1468.1 (m), 1417.4 (m), 1347.3 (s), 1072.9 (w), 1013.4 (w), 829.9 (m), 752.1 (w) cm<sup>-1</sup>.

**Complex 2:** This complex was synthesized following the same procedure as for complex **1** except the starting ligand was replaced by **L'**. Dark-purple single crystals suitable for X-ray diffraction were obtained by slow evaporation of the solvent. Yield 166 mg (82%). C<sub>16</sub>H<sub>20</sub>CuN<sub>3</sub>O<sub>3.50</sub>S (405.95): calcd. C 47.4, H 4.79, N 10.6; found C 47.0, H 4.76, N 10.5. IR (KBr):  $\tilde{\nu}$  = 3472.1 (m), 1685.1 (s), 1594.0 (s), 1571.8 (s), 1501.8 (m), 1467.4 (m), 1412.5 (s), 1206.3 (s), 1140.0 (m), 830.9 (m), 788.6 (w), 725.5 (w) cm<sup>-1</sup>.

**X-ray Crystallographic Study:** The main crystallographic data for ligand **L** and complexes **1** and **2** are summarized in Table 2. The crystals of ligand **L** and complex **1** were determined on a Siemens P4 four-circle diffractometer at 293 K. An empirical absorption correction was made ( $\psi$ -scan). The structure was solved by Patterson methods and completed by iterative cycles of least-squares

refinement and  $\Delta F$  syntheses. H-atoms were located in their calculated positions and treated as riding on the atoms to which they are attached. All non-hydrogen atoms were refined anisotropically. All calculations were carried out with the SHELXTL program.<sup>[33]</sup> The crystal of complex **2** was determined on a Siemens SMART CCD diffractometer at 293 K. The program SAINT<sup>[34]</sup> was used for data reduction and an empirical absorption correction was carried out using the SADABS program.<sup>[35]</sup> The structure was solved by Patterson methods that revealed the position of all non-hydrogen atoms and refined using the full-matrix least-squares method on  $F_{\text{obs}}^2$  with the SHELXTL software package.<sup>[33]</sup> All non-hydrogen atoms were placed in calculated positions. Atomic scattering factors and anomalous dispersion corrections were taken from ref.<sup>[36]</sup> CCDC-223042 (for **L**), -223043 (for **1**) and -223044 (for **2**) contain the supplementary crystallographic data for this paper. These data can be obtained free of charge at [www.ccdc.cam.ac.uk/conts/retrieving.html](http://www.ccdc.cam.ac.uk/conts/retrieving.html) [or from the Cambridge Crystallographic Data Centre, 12 Union Road, Cambridge CB2 1EZ, UK; Fax: +44-1223-336-033; E-mail: [deposit@ccdc.cam.ac.uk](mailto:deposit@ccdc.cam.ac.uk)].

**Cytotoxicity Assays:** The cytotoxicity assays of **L** and **L'** and their Cu<sup>II</sup> complexes **1** and **2** were performed as follows. Tumor cell lines were grown in RPMI-1640 medium supplemented with 10% (v/v) heat-inactivated fetal bovine serum, 2 mM glutamine, 100 U/mL penicillin, and 100 µg/mL streptomycin (GIBCO, Grand Island, NY) in a highly humidified atmosphere of 95% air with 5% CO<sub>2</sub> at 310 K.

The growth inhibitory effect on the murine leukemia P-388 cell line was measured by the microculture tetrazolium [3-(4,5-dimethylthiazol-2-yl)-2,5-diphenyltetrazolium bromide, MTT] assay.<sup>[37]</sup> Briefly, cells in 100 µL of culture medium were plated in each well of 96-

Table 2. Crystal data and structure refinement for ligand **L**, complexes **1** and **2**

	Ligand <b>L</b>	Complex <b>1</b>	Complex <b>2</b>
Empirical formula	C <sub>19</sub> H <sub>25</sub> N <sub>3</sub> O <sub>3</sub> S	C <sub>16</sub> H <sub>19</sub> CuN <sub>3</sub> O <sub>4</sub> S	C <sub>16</sub> H <sub>20</sub> CuN <sub>3</sub> O <sub>3.50</sub> S
Molecular mass	375.48	412.94	405.95
<i>T</i> (K)	293(2)	293(2)	293(2)
Crystal size (mm)	0.25×0.20×0.15	0.35×0.25×0.18	0.30×0.25×0.15
Crystal habit, color	block, colorless	prism, brownish-red	prism, dark purple
Crystal system	orthorhombic	orthorhombic	monoclinic
Space group	<i>P</i> 2 <sub>1</sub> 2 <sub>1</sub> 2 <sub>1</sub>	<i>P</i> 2 <sub>1</sub> 2 <sub>1</sub> 2 <sub>1</sub>	<i>C</i> 2
<i>a</i> (Å)	5.157(1)	5.556(1)	28.463(6)
<i>b</i> (Å)	19.052(4)	15.002(3)	5.264(1)
<i>c</i> (Å)	19.593(4)	20.886(4)	13.345(3)
$\beta$ (°)			109.142(3)
<i>V</i> (Å <sup>3</sup> )	1925.0(7)	1740.9(6)	1888.8(7)
<i>Z</i>	4	4	4
Calculated density (mg·m <sup>-3</sup> )	1.296	1.576	1.428
Absorption coefficient (mm <sup>-1</sup> )	0.192	1.401	1.288
<i>F</i> (000)	800	852	840
$\theta$ range for data collection (°)	1.49 to 25.00	1.67 to 24.96	1.82 to 27.98
Limiting indices	0 ≤ <i>h</i> ≤ 6 0 ≤ <i>k</i> ≤ 22 −23 ≤ <i>l</i> ≤ 23	0 ≤ <i>h</i> ≤ 6 0 ≤ <i>k</i> ≤ 17 0 ≤ <i>l</i> ≤ 24	−29 ≤ <i>h</i> ≤ 37 −6 ≤ <i>k</i> ≤ 6 −17 ≤ <i>l</i> ≤ 17
Reflections collected/unique	3867/3367 ( <i>R</i> <sub>int</sub> = 0.0388)	1801/1801 ( <i>R</i> <sub>int</sub> = 0.0025)	5608/3827 ( <i>R</i> <sub>int</sub> = 0.0513)
Absorption corrections	empirical	empirical	empirical
Data/restraints/parameters	3367/0/236	1801/0/226	3827/8/223
Goodness-of-fit on <i>F</i> <sup>2</sup>	1.066	1.023	1.046
Final <i>R</i> <sub>int</sub> [ <i>I</i> > 2σ( <i>I</i> )] <sup>[a]</sup>	<i>R</i> 1 = 0.0386, <i>wR</i> 2 = 0.1181	<i>R</i> 1 = 0.0375, <i>wR</i> 2 = 0.0933	<i>R</i> 1 = 0.1064, <i>wR</i> 2 = 0.2824
<i>R</i> <sub>int</sub> (all data) <sup>[a]</sup>	<i>R</i> 1 = 0.0614, <i>wR</i> 2 = 0.1604	<i>R</i> 1 = 0.0653, <i>wR</i> 2 = 0.1432	<i>R</i> 1 = 0.1225, <i>wR</i> 2 = 0.2941
Largest diff. peak, hole (e·Å <sup>-3</sup> )	0.210, −0.210	0.337, −0.374	2.052, −0.624

<sup>[a]</sup>  $R1 = \sum ||F_o| - |F_c|| / \sum |F_o|$ ;  $wR2 = [\sum w(F_o^2 - F_c^2)^2 / \sum w(F_o^2)^2]^{1/2}$ .

well plates (Falcon, Calif.). The cells were treated in triplicate with grade concentrations of the ligands, copper complexes and the reference drug cisplatin at 310 K for 48 h. A 20  $\mu\text{L}$  aliquot of MTT solution (5 mg/mL) was added directly to all the appropriate wells. The culture was then incubated for 4 h. Then 100  $\mu\text{L}$  of "triplex solution" (10% SDS/5% isobutanol/12 mM HCl) was added. After incubating the plates at 310 K overnight, they were measured by the absorbance at 570 nm using a multiwell spectrophotometer (VERSA Max, Molecular Devices, USA).

For the lung adenocarcinoma A-549 cell line, the growth inhibition was analyzed by the sulforhodamine B (SRB) assay.<sup>[38]</sup> Briefly, adherent cells in 100  $\mu\text{L}$  of medium were seeded in 96-well plates and allowed to attach for 24 h before drug addition. The cell densities were selected based on preliminary tests to maintain control cells in an exponential phase of growth during the period of the experiment and to obtain a linear relationship between the optical density (OD) and the number of viable cells. Each cell line was exposed to grade concentrations of the compounds at desired final concentrations for 72 h and each concentration was tested in triplicate wells. After exposure, cells were fixed by gentle addition of 100  $\mu\text{L}$  of cold (277 K) 10% trichloroacetic acid to each well, followed by incubation at 277 K for 1 h. The plates were washed with deionized water five times and allowed to dry in air. The cells were stained by addition of 100  $\mu\text{L}$  of SRB solution [0.4% SRB (w/v) in 1% acetic acid (v/v)] to the wells for 15 min. The plates were then quickly washed five times with 1% acetic acid to remove any unbound dye and allowed to dry in air. Bound dye was solubilized with 10 mmol·mL<sup>-1</sup> Tris (pH 10.5) prior to reading the plates. The OD value was read at a wavelength of 515 nm. Media and DMSO control wells, in which compounds were absent, were included in all the experiments. The growth inhibitory rate of treated cells was calculated by  $(\text{OD}_{\text{control}} - \text{OD}_{\text{test}})/\text{OD}_{\text{control}} \times 100\%$ .

**Spectral Studies of Interactions with DNA and GSH:** The concentration of DNA was determined by measuring the UV absorption at 260 nm and taking the molar absorption coefficient ( $\epsilon_{260}$ ) of CT-DNA as 6600 L·mol<sup>-1</sup>·cm<sup>-1</sup>.<sup>[39]</sup> Circular dichroism (CD) spectra were recorded on a Jasco J-810 spectropolarimeter. Each sample solution was scanned in the range 225–300 nm. A CD spectrum was generated which represented the mean of three scans from which the solvent background had been subtracted. The UV/Vis spectra of complexes **1** and **2** on addition of CT DNA were obtained on a UV-3100 spectrometer at a molar ratio (DNA/copper) of 0.0, 0.2, 0.4, 0.6. The UV/Vis spectroscopic titrations were carried out at room temperature by adding increasing amounts of GSH ( $0, 0.55 \times 10^{-5}, 0.83 \times 10^{-5}, 1.11 \times 10^{-5}, 1.67 \times 10^{-5}, 2.22 \times 10^{-5}, 3.33 \times 10^{-5}$  mol·L<sup>-1</sup>) to a solution of complexes **1** or **2** at a fixed concentration ( $3.33 \times 10^{-5}$  mol·L<sup>-1</sup>) contained in a quartz cell. The time span between two successive spectra was 10 min.

## Acknowledgments

We thank the financial support from the National Natural Science Foundation of China (No.s 20231010 and 20228102) and the Ministry of Education for Specialized Research Fund for the Doctoral Program of Higher Education (No. 20010284029).

<sup>[1]</sup> K. H. Thompson, C. Orvig, *Science* **2003**, *300*, 936–939.

<sup>[2]</sup> E. Wong, C. M. Giandomenico, *Chem. Rev.* **1999**, *99*, 2451–2466.

- <sup>[3]</sup> M. J. Clarke, F. C. Zhu, D. R. Frasca, *Chem. Rev.* **1999**, *99*, 2511–2534.
- <sup>[4]</sup> Z. J. Guo, P. J. Sadler, *Adv. Inorg. Chem.* **2000**, *49*, 183–306.
- <sup>[5]</sup> G. J. Brewer, *Curr. Opin. Chem. Biol.* **2003**, *7*, 207–212.
- <sup>[6]</sup> G. J. van Giessen, J. A. Crim, D. H. Petering, H. G. Petering, *J. Natl. Cancer Inst.* **1973**, *51*, 139–146.
- <sup>[7]</sup> J. Easmon, G. Pürstinger, G. Heinisch, T. Roth, H. H. Fiebig, W. Holzer, W. Jäger, M. Jenny, J. Hofmann, *J. Med. Chem.* **2001**, *44*, 2164–2171.
- <sup>[8]</sup> M. B. Ferrari, F. Bisceglie, G. Pelosi, P. Tarasconi, R. Albertini, P. P. Dall'Aglio, S. Pinelli, A. Bergamo, G. Sava, *J. Inorg. Biochem.* **2004**, *98*, 301–312.
- <sup>[9]</sup> A. De Vizcaya-Ruiz, A. Rivero-Muller, L. Ruiz-Ramirez, G. E. N. Kass, L. R. Kelland, R. M. Orr, M. Dobrota, *Toxicol. in Vitro* **2000**, *14*, 1–5.
- <sup>[10]</sup> I. Gracia-Mora, L. Ruiz-Ramirez, C. Gómez-Ruiz, M. Tinoco-Méndez, A. Márquez-Quinones, L. R. de Lira, A. Marín-Hernández, L. Macías-Rosales, M. E. Bravo-Gómez, *Met.-Based Drugs* **2001**, *8*, 19–28.
- <sup>[11]</sup> D. Y. Kong, C. Qin, L. H. Meng, Y. Y. Xie, *Bioorg. Med. Chem. Lett.* **1999**, *9*, 1087–1092.
- <sup>[12]</sup> I. Dovinová, H. Paulíková, P. Rauko, L. Hunáková, E. Hanušová, E. Tibenská, *Toxicol. in Vitro* **2002**, *16*, 491–498.
- <sup>[13]</sup> D. Y. Kong, A. E. Martell, R. J. Motekaitis, *Inorg. Chem.* **2001**, *40*, 298.
- <sup>[14]</sup> J. A. Broomhead, G. Camm, M. Sterns, L. Webster, *Inorg. Chim. Acta* **1998**, *271*, 151–159.
- <sup>[15]</sup> J. Y. Zhang, X. Y. Wang, C. Tu, J. Lin, J. Ding, L. P. Lin, Z. M. Wang, C. He, C. H. Yan, X. Z. You, Z. J. Guo, *J. Med. Chem.* **2003**, *46*, 3502–3507.
- <sup>[16]</sup> T. Yang, C. Tu, J. Y. Zhang, L. P. Lin, X. M. Zhang, Q. Lin, J. Ding, Q. Xu, Z. J. Guo, *Dalton Trans.* **2003**, *17*, 3419–3424.
- <sup>[17]</sup> J. Y. Zhang, X. K. Ke, C. Tu, J. Lin, J. Ding, L. P. Lin, H. K. Fun, X. Z. You, Z. J. Guo, *BioMetals* **2003**, *16*, 485–496.
- <sup>[18]</sup> R. L. Chapman, F. S. Stephens, R. S. Vagg, *Inorg. Chim. Acta* **1980**, *43*, 29–33.
- <sup>[19]</sup> J. M. Rowland, M. L. Thornton, M. M. Olmstead, P. K. Mascharak, *Inorg. Chem.* **2001**, *40*, 1069–1073.
- <sup>[20]</sup> J. Y. Zhang, Q. Liu, Y. Xu, Y. Zhang, X. Z. You, Z. J. Guo, *Acta Crystallogr., Sect. C* **2001**, *57*, 109–110.
- <sup>[21]</sup> Y. Shao, C. Tu, J. Y. Zhang, Z. J. Guo, *Acta Crystallogr., Sect. E* **2003**, *59*, 527–529.
- <sup>[22]</sup> D. X. West, H. Gebremedhin, R. J. Butcher, J. P. Jasinski, A. E. Liberta, *Polyhedron* **1993**, *12*, 2489–2497.
- <sup>[23]</sup> M. Akbar Ali, K. K. Dey, M. Nazimuddin, R. J. Butcher, F. E. Smith, J. P. Jasinski, J. M. Jasinski, *Polyhedron* **1996**, *15*, 3331–3339.
- <sup>[24]</sup> M. Akbar Ali, A. H. Mirza, R. J. Butcher, *Polyhedron* **2001**, *20*, 1037–1043.
- <sup>[25]</sup> A. Mohindru, J. M. Fisher, M. Rabinovitz, *Nature (London)* **1983**, *303*, 64–65.
- <sup>[26]</sup> E. W. Ainscough, A. M. Brodie, W. A. Denny, G. J. Finlay, J. D. Ranford, *J. Inorg. Biochem.* **1998**, *70*, 175–185.
- <sup>[27]</sup> E. R. Jamieson, S. J. Lippard, *Chem. Rev.* **1999**, *99*, 2467–2498.
- <sup>[28]</sup> P. A. Andrews, M. P. Murphy, S. B. Howell, *Cancer Chemother. Pharmacol.* **1987**, *19*, 149–154.
- <sup>[29]</sup> Y. T. Kang, M. D. Enger, *Toxicology* **1988**, *48*, 93–101.
- <sup>[30]</sup> T. Ochi, F. Otsuka, K. Takahashi, M. Ohswa, *Chem.-Biol. Interact.* **1988**, *65*, 1–14.
- <sup>[31]</sup> D. E. Conner, A. H. Ringwood, *Aquat. Toxicol.* **2000**, *50*, 341–349.
- <sup>[32]</sup> J. F. Jiang, C. M. S. Croix, N. Sussman, Q. Zhao, B. R. Pitt, V. E. Kagan, *Chem. Res. Toxicol.* **2002**, *15*, 1080–1087.
- <sup>[33]</sup> G. M. Sheldrick, *SHELXTL v5, Reference Manual*, Siemens Analytical X-ray Systems, Madison, WI. **1996**.

- [34] G. M. Sheldrick, *SAINT v4, Software Reference Manual*, Siemens Analytical X-ray Systems, Madison, WI. **1996**.
- [35] G. M. Sheldrick, *SADABS, Program for Empirical Absorption Correction of Area Detector Data*, University of Göttingen, Germany. **1996**.
- [36] A. J. Wilson, *International Table for X-ray Crystallography*, Kluwer Academic Publishers, Dordrecht. **1992**, vol. C, Tables 6.1.1.4 (p.500) and 4.2.6.8 (p. 219), respectively.
- [37] M. C. Alley, D. A. Scudiero, A. Monks, M. L. Hursay, M. J. Czerwinski, D. Fine, B. J. Abbott, J. G. Mayo, R. H. Shoemaker, M. R. Boyd, *Cancer Res.* **1988**, *48*, 589–601.
- [38] P. Skehan, R. Storeng, D. Scudiero, A. Monks, J. McMahon, D. Vistica, J. T. Warren, H. Bokesch, S. Kenney, M. R. Boyd, *J. Natl. Cancer Inst.* **1990**, *82*, 1107–1112.
- [39] M. E. Reichmann, S. A. Rice, C. A. Thomas, P. Doty, *J. Am. Chem. Soc.* **1954**, *76*, 3047–3053.

Received May 1, 2004

Early View Article

Published Online August 12, 2004